

MASSES, TIDAL RADII AND ESCAPE SPEEDS IN DWARF SPHEROIDAL GALAXIES UNDER MOND AND DARK HALOS COMPARED

F. J. SÁNCHEZ-SALCEDO AND X. HERNÁNDEZ

Instituto de Astronomía, Universidad Nacional Autónoma de México, Ciudad Universitaria, Apt. Postal 70
264, C.P. 04510, Mexico City, Mexico

jsanchez@astroscu.unam.mx, xavier@astroscu.unam.mx

Draft version November 4, 2018

ABSTRACT

We investigate the success and problems of MODified Newtonian Dynamics (MOND) in explaining the structural parameters and dynamics of remote Galactic globular clusters (GCs) and dwarf spheroidal (dSph) galaxies. Using the MOND value for the mass of the Milky Way as inferred from the Galactic rotation curve, we derive the tidal radii of Galactic GCs, and compare to observed values. Except for Pal 14, the predicted tidal radii of GCs are systematically larger than the observed nominal values. However, the associated uncertainties are so large that tidal radii are consistent on the 1σ level. We have considered the importance of the Galactic tidal force on the survival of dSphs under MOND. Assuming mass-to-light ratios compatible with a naked stellar population, we found that the present Galactic dSphs preserve their integrity over one Hubble time, except Sextans which may survive the tidal interaction only for several Gyr. Mass-to-light ratios as inferred from the internal kinematics of dSph galaxies can be used, but they appear too large to be accounted for only by the stellar population in Willman 1, Coma Berenice, Ursa Minor, Draco, Ursa Major and possibly Boötes dwarves. Finally, the ability of the Sculptor dwarf to retain the observed population of low-mass X-ray binaries (LMXBs) is examined. Under the MOND paradigm, we find that the retention fraction in Sculptor is likely not larger than a few percent. Compared to the dark matter scenario, it turns out that MOND makes the retention problem worse. We propose that measurements of the radial velocities of the observed LMXBs in Sculptor could provide a way to distinguish between modified gravities or extended and massive dark matter halos.

Subject headings: galaxies: dwarf – galaxies: individual (Sculptor) – galaxies: kinematics and dynamics – gravitation

1. INTRODUCTION

The dynamical mass-to-light ratios, M/L , derived in galaxies are usually larger than the expected mass-to-light ratio of the stellar component, usually interpreted as indicating that they must contain dark matter. Alternatively, one could argue that the discrepancy between total mass and baryonic mass is telling us that the Newtonian law of gravity is not governing the dynamics. In particular, the MODified Newtonian Dynamics (MOND) proposed by Milgrom (1983) has been proven to be successful in explaining how galaxies rotate, without any dark matter (see Sanders & McGaugh 2002 for a review). It is important to note that MOND ideas and variants have so far been introduced, tailored and calibrated with the explicit objective of accounting for the first order gravitational effects of hypothetical dark matter halos: rotation curves in large galaxies and stellar velocity dispersions in spheroidal systems. One should also note that a wide range of other gravitational effects appear in galactic dynamics, which in principle, offer independent restrictions on any proposed modified dynamic scheme. Some examples include the gravitational stability of galactic disks (e.g., Sánchez-Salcedo & Hidalgo-Gómez 1999) or relaxation processes in stellar systems (Ciotti & Binney 2004). Concerning dSphs, in Sánchez-Salcedo et al. (2006) we investigated the effects the enhanced gravitational relevance of the stellar population under MOND would have upon the problem of the orbital decay of globular clusters (GCs) due to dynamical friction, and found that although such a proposal can account for the velocity dispersion measurements, in-

spiraling times become uncomfortably short.

Gerhard & Spergel (1992) and Gerhard (1994) derived the mass-to-light ratios in MOND for seven dwarfs from virial arguments. Later on, Milgrom (1995) reanalyzed the M/L values with new data. He concluded that when uncertainties in the observed luminosity and central velocity dispersion are included, the values agree with those expected for a normal old stellar population. The flux of data about the kinematics of Local dSphs is growing rapidly. The new determinations of line-of-sight velocity profiles, the recent discovery of a dozen dSph galaxies, and the detection of low-mass X-ray binaries (LMXBs) in Sculptor may give crucial clues on the dark matter problem and its alternatives. In the Newtonian approach, these observations lend support to the cosmological-motivated interpretation that some dSphs reside within the most massive and extended substructure dark matter halos (Kleyna et al. 2001, 2005; Dehnen & King 2006). The fact that some dSph galaxies possess two distinct populations, as inferred from studies of resolved stellar populations, e.g. Hernandez et al. (2000) for Carina and Leo I, also suggests an extended dark matter halo in order to prevent the loss of all the gas during the first starburst. The question that arises is whether MOND can mimic an extended halo in dSphs or not. Lokas (2002) and Lokas et al. (2006) have noticed that MOND experiences a serious difficulty in explaining the velocity dispersion profile of Draco without dark matter.

A wide view of the successes and problems of MOND in dSph galaxies in comparison to the dark matter scenario can motivate new tests on the nature of dark matter

and its alternatives. Here we will investigate the ability of MOND in explaining the observed tidal radii in Galactic GCs and dSph galaxies (§2), and the problem of the retention of LMXBs in dSphs (§3), within the alternative optics of MOND without dark matter. As a byproduct, an updated compilation of the mass-to-light ratios in satellite dSphs under MOND is given.

2. TIDAL RADII OF GCs AND THE SURVIVAL OF DSPHS

In any law of gravity, the global M/L ratio in a spherical system can be derived in different ways; either modeling the observed velocity dispersion profile of the stars or using the observed King tidal radius. The observed tidal radii can provide lower limits for the M/L that are independent of kinematic data (e.g., Faber & Lin 1983; Oh, Lin & Aarseth 1995; Pryor 1996; Burkert 1997; Walcher et al. 2003).

The dynamical King (1962) tidal radius of a GC or a dSph orbiting in a circular orbit of radius D around a galaxy with a logarithmic potential is defined as:

$$r_t = k \left[\frac{M_{dw}}{2M_G(D)} \right]^{1/3} D, \quad (1)$$

where M_{dw} is the mass of the satellite, $M_G(D)$ the host galaxy mass inside D and k is Keenan's (1981a,b) factor, which depends on the gravity law, and accounts for the elongation of the zero-velocity surface along the line joining the cluster and galactic centers. For eccentric orbits,

$$r_t = ka \left[\frac{M_{dw}}{M_G(a)} \right]^{1/3} \left[\frac{(1-e)^2}{[(1+e)^2/2e] \ln [(1+e)/(1-e)] + 1} \right]^{1/3}, \quad (2)$$

where e and a are the orbital eccentricity and the semi-major axis, respectively. This formula for the tidal radius is valid for both Newtonian (e.g., Oh, Lin & Aarseth 1992) and MOND gravities (Gerhard & Spergel 1992; Baumgardt, Grebel & Kroupa 2005; Zhao & Tian 2006) provided that the masses and the Keenan factor are taken appropriately. In the MONDian case without dark matter, M_{dw} and M_G are the "true" baryonic masses of the dSph satellite and the host galaxy, respectively. Knowing the Galactic mass radial profile and the eccentricity e and by equating King's tidal radius, r_t , with the observed limiting radius, a lower limit on M/L of the satellite system can be inferred.

The nominal value $k = 1$, as first suggested in King's paper (1962), corresponding to the distance of the last closed zero-velocity surface along the line joining the center of the galaxy with the center of the satellite system, is commonly adopted as a useful fiducial length scale under Newtonian gravity, after the work of Oh, Lin & Aarseth (1992) and Oh, Lin & Aarseth (1995), who demonstrated that even in the absence of significant two-body relaxation processes, the density profile of GCs in circular orbit resembles the King-Michie model with an asymptotic limiting radius consistent with the tidal radius as defined by King (1962), with $k = 1$. If we adopt the same definition of tidal radius in MOND, i.e. the distance to the zero-velocity surface along the axis pointing in the radial direction, we also get $k = 1$ (Zhao & Tian 2006).

The parameter F , defined as the ratio between the observed cutoff radius and the dynamical tidal radius as

defined in Eq. (2) with $k = 1$, is a useful indicator of the importance of the Galactic tidal force on the internal structure of GCs and dSphs (Oh, Lin & Aarseth 1995; Piatek & Pryor 1995). For values $F < 1$, the tidal force is unable to stretch the satellite object significantly, and only internal processes may be considered. In this case, the stellar component of the dSph galaxies is not tidally truncated, and mass estimators based on the tidal radius underestimate the total M/L substantially. At values $F \sim 2$, a dSph can survive the tidal interaction for several Gyr. At these values a dSph could actually be unbound but not yet dispersed, as the timescales for disruption exceed several Gyrs. With the effect of the force increasing rapidly with increasing F , for $F \sim 3$ the satellite disintegrates in a few orbits. Since it is unlikely that we are observing satellites in such a short-lived evolutionary state (except Sagittarius), $F < 2$ is expected.

The values of F under MOND, F_M , for Galactic GCs and satellite dSphs have been calculated recently by Zhao (2005). Zhao (2005) uses a Keenan factor $k = \sqrt{2}/3$ and equates the mass ratio with the luminosity ratio, i.e. $M_{dw}/M_G \approx L_{dw}/L_G$ in Eq. (1), where L_{dw} and L_G are the luminosities of the dwarf galaxy and our Galaxy, respectively. The large scatter found in the values of F_M was interpreted by Zhao (2005) as challenging for any baryonic MOND Universe.

In this Section, we revisit the consistency of the predictions of MOND with observations using the tidal radius theory, assuming the mass of the Milky Way to be known. We discuss GCs (§2.1) and dSphs (§2.2) separately, since remote GCs are likely tidally truncated, whereas dSph galaxies are not necessarily tidally truncated, even though their luminosity profiles can be fitted by King models.

2.1. Globular clusters

In order to estimate the tidal radii of Galactic globular clusters under MOND, we must start by adopting a mass model for the Milky Way under MOND. We take this from Famaey & Binney (2005) (their model I) who use the Galactic rotation curve, over the region where it is well measured, the first 10 kpc, to derive a total baryonic mass of $M_G = 0.6\text{--}0.8 \times 10^{11} M_\odot$ (see also Dehnen & Binney 1998). This yields a circular rotation at the solar circle of 200 km s^{-1} and good agreement with dynamical measurements at all radii internal to 10 kpc. Since the asymptotic circular velocity of test particles around a mass M_G is $V = (GM_G a_0)^{1/4}$, this implies an asymptotic circular velocity of $170 \pm 5 \text{ km s}^{-1}$ (essentially shared by most of their models, see also Famaey et al. 2007), for our adopted $a_0 = 0.9 \times 10^{-8} \text{ cm s}^{-2}$, which is the value derived in Begeman et al. (1991) rescaled to the new distance scale (Bottema et al. 2002). This mass compares quite well with the expected baryonic disk mass for a galaxy with a disk V band luminosity of $\sim 1.5 \times 10^{10} L_{\odot,V}$. The asymptotic value of the rotation curve might seem a little on the low side, but one must bear in mind that more familiar values of order of 200 km s^{-1} are the result of extrapolating dark halo mass models beyond the regions where the rotation curve as such is actually measured.

It is worthwhile to compare the King tidal radii in the Newtonian dark matter scenario and in MOND. According to Eq. (1), the tidal radius in the conventional dark mat-

ter model depends on the total mass of the host galaxy as $[M_{G,bar}(D) + M_{G,dm}(D)]^{1/3}$, where $M_{G,bar}$ and $M_{G,dm}$ are the baryonic and dark mass, respectively. In MOND, the tidal radius goes as $[M_{bar}(D)]^{1/3}$, where M_{bar} is the baryonic mass only. So that, remote GCs (those at $D > 35$ kpc) should be the best discriminators between MOND and Newtonian dynamics as the dark halo mass becomes significant at large distances.

Unfortunately, the range $D > 35$ kpc is mainly populated by sparse, low-luminosity clusters with rather uncertain tidal radii and integrated magnitudes. For illustration, for NGC 2419, which is the fourth most luminous cluster of the Galaxy, discrepant values for the global M/L and cutoff radius can be found in the literature. Pryor & Meylan (1993) report $M/L = 1.2$ and $r_t = 230$ pc (see also Trager et al. 1995), whereas Olszewski et al. (1993) derive a global M/L ratio of 0.7 ± 0.4 and $r_t = 280$ pc. As discussed in detail by Wakamatsu (1981), Innanen et al. (1983) and Bellazzini (2004), who estimate M_G under Newtonian dynamics using the tidal radii of remote GCs, the observed tidal radii are affected by large uncertainties. The conventional method for determining the tidal radii involves a large outward extrapolation of the surface brightness profile. Innanen et al. (1983) suggest random errors of a factor ~ 2 in r_t . Moreover, the adoption of different models to fit them may lead to significantly larger limiting radii than estimated with King's models (McLaughlin & Meylan 2003). Our first objective is to test MOND using the observed tidal radii of remote GCs, including fully all the sources of uncertainty in the analysis.

The complete list of known GCs beyond 35 kpc until 2006 is Pal 2, Pal 15, NGC 7006, Pixis, Pal 14, NGC 2419, Eridanus, Pal 3, Pal 4 and AM-1 (Harris 1996). However, Pal 2, Pal 15 and Pyxis are not suited for the present study because they are strongly affected by extinction. Two new extremely low luminosity GCs have been discovered recently (Koposov et al. 2007), but the number of stars detected is not enough to measure precisely their luminosities and tidal radii.

Those GCs with orbital periods, P , much shorter than the half-mass internal relaxation time, t_{rh} , are expected to be limited by Galactic tides at perigalacticon, because internal relaxation is unable to restore a larger limiting radius before the next perigalactic passage (e.g., Oh et al. 1995). In clusters with an orbital period similar or larger than the relaxation time, internal relaxation is able to repopulate their external regions after perigalacticon passage and their tidal radii may be comparable to the instantaneous theoretical value and, hence, values $F \sim 1$ are expected (Bellazzini 2004). For the remote GCs of our sample from which orbital parameters are available, NGC 7006 and Pal 3, have $P/t_{rh} \sim 1$ (Harris 1996). Therefore, we can be certain that they have $F \sim 1$. Eridanus and AM-1, situated at a galactocentric distance of ~ 95 kpc and 123 kpc, respectively, are likely limited by the Galactic tidal force at its present position because their t_{rh} value ≈ 2.5 –5 Gyr is short compared to their orbital periods. In the case of NGC 2419, $t_{rh} \approx 35$ Gyr. Hence, it should be limited by Galactic tides at perigalacticon. Finally, P/t_{rh} is difficult to infer for Pal 14 and Pal 4. We

consider as a working assumption that the observed tidal radii of distant GCs, except for NGC 2419, are probes of the Galactic tidal force at their present position, bearing in mind that we may overestimate r_t for Pal 14 and Pal 4. The predicted r_t values are estimated according to Eq. (1) for all GCs, except NGC 2419, in a MOND model where the Galactic mass is fixed by the inner rotation curve.

For NGC 2419 we are forced to assume an orbital eccentricity. Since its orbital parameters are unknown we will follow a statistical procedure. For the 48 GCs with determinations of the orbital parameters, $e = 0.5 \pm 0.25$ at the 1σ level (Allen, Moreno & Pichardo 2006). Therefore, we will estimate r_t for NGC 2419 using Eq. (2) and an eccentricity taken as a most likely value of 0.5, with a 1σ uncertainty of 0.25. We should note that there is a trend on the eccentricity with their apogalacticon distance: most GCs with apogalacticon distances $\lesssim 10$ kpc have eccentricities between 0 and 0.6, whereas those with apogalacticons $\gtrsim 10$ kpc the eccentricities are populated mainly in the interval 0.4–1.0. Therefore, adopting $e = 0.5 \pm 0.25$ we are overestimating the upper error range on r_t since the eccentricity of NGC 2419 is likely > 0.4 .

When estimating r_t from Eqs. (1) or (2), D is derived from the distance modulus μ_V , the color excess $E(B - V)$ and the galactic coordinates, whereas the mass of the cluster is derived from the apparent integrated V -magnitude V_t , μ_V and the stellar mass-to-light ratio M/L . Reddening correction, though small (less than 0.1 mag in the color excess for all of the GCs considered), was taken into account. As said before, in order to quantify the success or failure of MOND in explaining the measured tidal radii of GCs, we should include the associated uncertainties in the analysis: there are dispersions around μ_V , V_t , M/L and Keenan's factor. We will proceed adopting the same associated uncertainties on input parameters as Bellazzini (2004) and are briefly described below.

(i) The mean values of μ_V and V_t were extracted from Harris (1996). The standard deviations for both μ_V and V_t were taken of 0.1 mag for NGC 2419 and NGC 7006 and 0.2 mag for the remaining clusters. The errors in μ_V are thought to account for both the measurement errors and the uncertainties affecting the distance scale of GCs (Cacciari 1999; Bellazzini 2004). No scatter was associated to the color excess; it was kept fixed for each GC.

(ii) The M/L values follow a truncated Gaussian distribution with a mean value of 1.2 and a standard deviation of 0.4, so that $M/L = 1.2 \pm 0.4$. The distribution is truncated at $M/L = 0.5$ (e.g., Pryor & Meylan 1993; Feltzing et al. 1999; Parmentier & Gilmore 2001).

(iii) The MONDian Keenan factor k is extracted from a uniform distribution bracketed by the intermediate and radial Roche radii, i.e. $0.35 < k < 1.0$. In fact, detailed analysis of the tidal radii of Galactic GCs in the Newtonian case¹ suggest that the Newtonian k values must vary from cluster-to-cluster in the range $0.5 \leq k \leq 1.0$ (e.g., Bellazzini 2004), probably because there are several mechanisms that induce an outward migration of stars and the escape of all extra-tidal stars is by no means assured. Therefore, it turns out that the possible k values are bracketed by the intermediate and radial Roche radii, which translates into $0.35 < k < 1.0$ in MOND.

¹ Note that GCs are supposed to contain no dark matter in these studies.

The inferred tidal radii with 1σ error bars for $M_G = 0.7 \times 10^{11} M_\odot$ (see §2.1) are shown in Fig. D1. For comparison, the observed limiting radii are also included. From inspection of the quality and extent of the surface brightness profile, Bellazzini (2004) assigns a standard deviation for the observed r_t values of 10% for NGC 2419, 20% for NGC 7006 and 30% for the remaining clusters. However, estimates of the tidal radii of Pal 3 and AM-1 have been superseded by Hilker (2006). Hence we have adopted these updated values with an uncertainty of 20%. It can be seen that the central predicted values are systematically larger than the observed values except for Pal 14. As anticipated, however, the uncertainties are so large that it is not possible to rule out MOND at all. The most problematic cases are Pal 3 and Pal 4, for which there is little overlap between the error bars. However, since the observed cutoff radii are plagued with systematic errors (e.g., Heggie & Ramamani 1995; McLaughlin & Meylan 2003; Bellazzini 2004), not included in the present analysis, we conclude that the present observational data does not allow us to distinguish between MOND and dark matter halos. If future more refined measurements simply reduce error bars, leaving central inferred values unchanged, tidal radii of GCs will indeed rule out MOND.

The differences between our conclusion and those of Zhao (2005) are probably due to the fact that we included all relevant sources of uncertainties in the problem, and to having modeled each GC using the observed M/L (with their uncertainties), rather than taking a generic value.

In the following section we shall extend the previous analysis of globular clusters to the case of dSph galaxies and evaluate the importance of the Galactic tide on their structure, which provide a new test for MOND.

2.2. Dwarf spheroidal galaxies

dSph galaxies are not necessarily tidally truncated systems because the timescale for two-body relaxation, which is ultimately responsible for the diffusion of stars to the outskirts of the dSph galaxy, may be so large that internal relaxation would be unable to smooth any hypothetical sharp edge in the stellar luminosity profile in one Hubble time. In the case of the remote Leo II dSph, for instance, the two-body relaxation timescale is > 300 Gyr even under modified dynamics (derived using Eq. 42 in Ciotti & Binney 2004 with a ratio between dark matter and luminous matter of $\mathcal{R} \approx 20$) and, hence, the fractional mass-loss rate $M_{dw}^{-1} dM_{dw}/dt \leq -0.045/t_{rh} \approx -1.5 \times 10^{-4}$ Gyr $^{-1}$ (Gnedin et al. 1999), is so small that the photometric contribution of unbound stars would be gone in the process of subtraction of the background population.

We have selected all the Milky Way satellites placed at $40 < D < 260$ kpc with determinations of their internal dynamics: strong candidates of the satellite companions to the Milky Way, namely Ursa Major II, Segue 1, Leo T and Boötes II dwarves are excluded. Canes Venatici I is also excluded because its complex dynamical structure would require a more sophisticated analysis (Ibata et al. 2006) and Leo IV because the kinematic data available is still very poor. The observed limiting radii were taken from Irwin & Hatzidimitriou (1995, henceforth IH95).

The predicted tidal radii under MOND theory were derived from Eq. (1) using $M_G = 0.7 \times 10^{11} M_\odot$ once M_{dw}

is known. We have estimated M_{dw} in two different manners. In a MONDian world, the dynamical mass is fully determined by the stars. If a value $M/L = 3$, corresponding to a normal old stellar population, is assumed for all the dSphs, then $F_M < 1.25$ for all of them except for Sextans, whose value is $F_M = 2.1$. This indicates that in order to have $F_M < 2$ for all galaxies, we should invoke a $M/L \sim 4$. Are these values of M/L consistent with their internal kinematics? In order to answer this question, the MOND M/L values, $(M/L)_M$, were inferred from the internal dynamics of the stars based on the most recent data.

Milgrom (1995) defined a parameter $\eta \equiv 1.5(\sigma/V)^2(D/r_c)$, with σ the stellar velocity dispersion of the dwarf, r_c its core radius, and V the galactic rotational velocity at D , which coincides with the asymptotic rotation velocity V_∞ for all the dwarfs. When $\eta \gg 1$, the dwarf can be treated as an isolated system and the global M/L was obtained exploiting a simple relation between the total mass M and the mean line-of-sight velocity dispersion, σ , in the isotropic, deep MOND case:

$$M = \frac{81}{4} \frac{\sigma^4}{G a_0} \quad (3)$$

(Gerhard & Spergel 1992; Milgrom 1994). When $\eta \ll 1$ and all accelerations relevant to the dwarf dynamics are smaller than a_0 , the dynamics becomes quasi-Newtonian. The MOND M/L for an object in the quasi-Newtonian regime can be obtained immediately from its Newtonian estimate,

$$\left(\frac{M}{L}\right)_M = \left(\frac{g_{\text{ext}}}{a_0}\right) \left(\frac{M}{L}\right)_N, \quad (4)$$

where g_{ext} is the acceleration of the system in the external field. We must notice, however, that due to the fact that the acceleration becomes anisotropic (Appendix A), the above relation is not strictly exact. Some idea of the uncertainty can be gained from the case of a homogeneous sphere, which we derive in Appendix B. The mass-to-light ratio in that ideal case is underestimated by a fraction $\sim 30\%$ (Appendix B) and, hence, due to the uncertainties in the structural parameters of these galaxies, this error is unimportant. For an isolated spherical system in the deep MOND limit, the central, MOND M/L value, $(M/L)_{0,M}$, as a function of the Newtonian estimator $(M/L)_{0,N}$ is given by:

$$\left(\frac{M}{L}\right)_{0,M} = 1.23 \left(\frac{\sigma_0^2}{a_0 r_c}\right) \left(\frac{M}{L}\right)_{0,N}, \quad (5)$$

with σ_0 the central velocity dispersion and r_c the core radius (Gerhard & Spergel 1992).

In Appendix C we briefly describe the observational parameters used to infer the mass-to-light ratios for each galaxy individually. Boötes, Sculptor, Sextans and Hercules have been assumed to be in the quasi-linear Newtonian regime, whereas the rest of the dSph were treated in the isolated limit. The derived global $(M/L)_N$ and $(M/L)_M$ are listed, when available, in Table D1, with $a_0 = 0.9 \times 10^{-8}$ cm s $^{-2}$ (Bottema et al. 2002; see §2.1) and the updated luminosities. For Coma Berenices, Boötes, Ursa Major, Hercules and Canes Venatici II, the values reported correspond to the central mass-to-light ratios. When the derived $(M/L)_M$ ratios lie within the range $0.5 < (M/L)_M < 12$, they might be in agreement

with a ‘naked’ old stellar population (Queloz et al. 1995; Romanowsky et al. 2003). Only when the resulting value is well out this range, we provide a lower limit at the 2σ confidence level, assuming that dSph galaxies have an isotropic velocity distribution; corrections for this are of as much as a factor 2. We wish to know if when assuming these lower 2σ limits on $(M/L)_M$, it also holds that $F_M < 2$. However, the reader interested in the mean $(M/L)_M$ values is referred to Appendix C.

The observed values of the limiting radii inferred by IH95 were used to derive F_N and F_M since they are usually adopted as the nominal values. The observed r_t in a certain galaxy may depend on the type of stars selected for its determination. For instance, red giant branch stars (RGB) are significantly less centrally condensed than the blue horizontal branch population in Sculptor (Westfall et al. 2006). More importantly, recent studies in some dSphs find a “break” in the King profile. The population beyond the break radius must signify either the presence of an extremely broad distribution of bound stars or the presence of unbound tidal debris (e.g., Westfall et al. 2006). In the latter case, r_t should be identified with the break radius. For Ursa Minor, Sculptor, Draco, Fornax and Leo I, we have listed additional rows in Table D1 with new determinations of r_t and luminosity. For conciseness, however, we do not give all the possible combinations of r_t and L but only the most relevant to assess the influence of observational uncertainties.

The derived values of F_M suggest that Leo I is the least likely to be affected by tidal effects. On the opposite side, Ursa Minor, Sculptor and Sextans may have $F_M \gtrsim 1$. Is there any evidence of the tidal distortion in these galaxies?

From photometric data of Ursa Minor, Palma et al. (2003) suggest that this object is evolving significantly because of the tidal influence of the Milky Way, although they cannot determine if the extra-tidal stars are now really unbound. In the case of Sculptor, the resultant value $F_M = 0.8\text{--}1.1$ is in perfect agreement with its appearance (see Section 3.1). We turn now our attention to Sextans. Applying Eq. (1) with $k = 1$, $M/L = 12$, $D = 86$ kpc and $M_G = 0.7 \times 10^{11} M_\odot$, we obtain $r_t = 2.15$ kpc. This value should be compared with that reported by IH95 (Table D1) to obtain $F_M = 1.3 \pm 0.5$, compatible with the requirement $F \leq 2$. We suggest that deep observations of Sextans, both photometrically and spectroscopically, out to radii larger than those where tails are detectable, may provide a test of MOND. If it is confirmed that Sextans is not being tidally distorted, this galaxy may need an extended halo of dark matter even under MOND dynamics. If so, the appeal of MOND would appear to be significantly weakened. In the standard Newtonian dark matter scenario $F_N = 1.4$ in Sextans, but it is likely that the global $(M/L)_N$ is larger than the quoted value of ~ 100 (Kleyna et al. 2004).

Finally, Draco, which has a large kinematic $(M/L)_M$, would survive the Galactic tide even if a $(M/L)_M = 2$, typical of an old stellar population, was adopted.

We conclude that it is very difficult at present to use the tidal radii of dSphs to distinguish between MOND and standard CDM. Until kinematic measurements definitively identify the tidal radii, the tidal approach should be treated with caution, as it is only an indicator of the

importance of the Galactic tidal force on the structure. In MOND, the dynamical M/L are systematically larger than the M/L inferred using the tidal radii (i.e. the requirement $F_M < 2$). Therefore, explaining the internal dynamics is a more profound question than the tidal radii. In fact, the high $(M/L)_M \gtrsim 20$ values required in Willman 1, Coma Berenice, Ursa Minor, Draco, Ursa Major and possibly Boötes are difficult to accept if MOND is a valid alternative to dark matter in dSph galaxies. Willman 1, Coma Berenice and Ursa Major are unique targets to test the success or failure of modified gravities at galactic scales. One could argue that an appropriate choice of anisotropy in the orbits of stars within these galaxies could reduce somehow these estimates. However, Lokas (2002) found the opposite trend in Draco and Fornax.

The relation between M/L and luminosity is shown in Figure D2 for our sample of galaxies. This figure is based on that given in Mateo et al. (1998) but for MOND. Even with considerable scatter, the clear trend between M/L and luminosity is because MOND is based on a characteristic acceleration and dSph galaxies present a characteristic velocity dispersion. According to this relation, the kinematics of the faintest dSph galaxies will be puzzling under MOND.

Galactic tides could, in principle, affect the kinematics and the apparent M/L derived from kinematic studies that assume dynamical equilibrium. For instance, Kuhn & Miller (1989) and Kroupa (1997) presented tidal models to explain large values of M/L in dwarf galaxies without resorting to dark matter. However, there is growing evidence that galactic tides cannot inflate the global M/L values: tides produce large ordered motions rather than large random motions (Piatek & Pryor 1995). Oh et al. (1995) found that the unbound but not yet dispersed systems have velocity dispersions that are comparable to the virial equilibrium value prior to disruption. Therefore, if the measurements do not seriously overestimate the velocity dispersion, either the mentioned galaxies are not in dynamical equilibrium due to recent gas mass loss or to a major merger with another dwarf galaxy, undergoing still a relaxation process, or they contain large amounts of dark matter even under modified dynamics. We believe that it is unlikely that the gas has been stripped from these galaxies only very recently, in the last few internal crossing-times. In particular, the fact that Draco and Ursa Minor have only very old stellar populations ($\gtrsim 10$ Gyr), suggests that they have possessed a dynamically-negligible fraction of mass in gas since a long time ago (Mayer et al. 2007).

3. RETENTION OF LOW-MASS X-RAY BINARIES

Recently, Dehnen & King (2006) have suggested that in order for Sculptor to retain the population of low-mass X-ray binaries observed by Maccarone et al. (2005) an extended dark matter halo of $\geq 10^9 M_\odot$ is required, i.e. $(M/L)_N \sim 600$. Here we explore the implications of this observation in order to see if the stronger gravity due to the stars alone under MOND also has the ability of retaining the observed LMXBs or not.

3.1. *The Sculptor dwarf spheroidal: Internal parameters and proper motion*

The Sculptor dSph is a satellite galaxy of the Milky Way, which presents a luminosity $(1.4 \pm 0.6) \times 10^6 L_\odot$ (IH95). According to the proper motion measurements by Piatek et al. (2006), it is on a polar orbit with apogalacticon at 122 kpc and perigalacticon at 68 kpc. The current galactocentric distance of Sculptor is 79 ± 4 kpc (Mateo 1998). A King model profile of limiting radius $79'.6 \pm 3'.3$, corresponding to 1.85 kpc and core radius $7'.14 \pm 0'.33$ (165 pc), fits the density profile well out to $60'$. Beyond this radius, a break population, which extends up to $150'$, has been found (Westfall et al. 2006). The ellipticity of the iso-density contours increases with increasing projected radius from the center of the dSph, from rounder to a value 0.32 in the outermost region (IH95; Westfall et al. 2006). Since there is no evidence for rotation, this flattening should be due to anisotropy in the velocity distribution, but it may also indicate that Sculptor is tidally distorted.

There is evidence that Sculptor contains two distinct ancient (both $\gtrsim 10$ Gyr old) stellar components. Tolstoy et al. (2004) derive different velocity dispersions for Sculptor stars separated into metallicity groups. The line-of-sight velocity dispersion of the metal-rich component is $\approx 7 \pm 1$ km s $^{-1}$, which is similar to the central line-of-sight velocity dispersion in Sculptor 6.2 ± 1.1 km s $^{-1}$ (Queloz et al. 1995; Westfall et al. 2006). Interestingly, the metal-poor component has a velocity dispersion of $\approx 11 \pm 1$ km s $^{-1}$ (see also Clementini et al. 2005). Westfall et al. (2006) derive a global velocity dispersion of 8.8 ± 0.6 km s $^{-1}$, which is intermediary to those that Tolstoy et al. (2004) report for these metallicity-separated populations. In the following, we will take the latter value as the mean line-of-sight velocity dispersion within the core, σ_c . From Fig. 12 in Westfall et al. (2006), one can see that it is a generously taken value.

3.2. *Escape velocity in the quasi-Newtonian MOND limit: Sculptor as a reference case*

The effective gravitational mass of a isolated galaxy under MOND increases linearly with R , and hence, any test particle is bound to the potential. However, due to the nonlinearity of the MOND field equation, for a satellite system situated in an external gravitational field, there exists a radius at which particles are stripped from the dSph by the tidal field of the host galaxy (see §2). For certain binary kick velocities, the LMXB system could become unbound from the gravitational potential of the satellite. Our aim in this Section is to estimate the kick velocity of a presupernova binary necessary to acquire the escape velocity, denoted by \vec{v}_k . In Sculptor, the calculation greatly simplifies because of the following reasons. It can be seen that the internal acceleration $\sim 1.6\sigma^2/r_c \sim 2 \times 10^{-9}$ cm s $^{-2}$ felt by a star in the core of Sculptor is significantly smaller than a_0 and thus, for the dynamics of an object in Sculptor the deep MOND regime would apply. In addition, the parameter η is $\lesssim 0.8$ for $V \gtrsim 185$ km s $^{-1}$. Since the internal acceleration goes as $\propto r$ at small radii and as $\lesssim r^{-1}$ at large radii, this value of η points to domination of the external field throughout the dwarf galaxy for $V \gtrsim 185$ km s $^{-1}$ (see also Milgrom 1995). At $V = 170$ km s $^{-1}$, we get $\eta \approx 1$, implying it is in the borderline of isolation with respect to the external acceleration field. Neither limit is valid in this case but the two limits should give similar

values for the escape speed.

A rough derivation of the escape speed follows; a more detailed calculation is presented in Appendix D. Suppose that a certain dSph can be described by a one-component King model (i.e. mass follows light). Then, the mass profile can be parameterized by W_0 , ρ_0 and r_c , with ρ_0 the total mass density at the center. In Newtonian dynamics, W_0 is the depth of the potential in units of the square velocity-dispersion parameter $\hat{\sigma}^2 \equiv 4\pi G\rho_0 r_c^2/9$. The escape velocity at any position is, therefore, smaller or equal to the central escape velocity $\sqrt{2W_0\hat{\sigma}^2}$. For the Galactic dSphs, W_0 lies in the range $2 < W_0 < 5$.

Consider now what happens under MOND theory. If this galaxy is in the quasi-Newtonian regime and MOND has the ability of reproducing the dynamics of this galaxy without dark matter, the depth of the potential under MOND must be similar to that in the case of the Newtonian dark matter scenario. Hence the central escape velocity is also $\sqrt{2W_0\hat{\sigma}^2}$ under MOND. In the case of Sculptor $W_0 \approx 4$ (IH95; Walcher et al. 2003; Westfall et al. 2006). For this value of W_0 , the velocity-dispersion parameter is related to the observed velocity dispersion within the core through $\hat{\sigma} = 1.16\sigma_c$ (see Fig. 4-11 in Binney & Tremaine 1987). Adopting $\sigma_c = 8.8$ km s $^{-1}$ (see §3.1), the central escape velocity in Sculptor under MOND is $\simeq \sqrt{10.8\sigma_c^2} = 29$ km s $^{-1}$.

The escape speed depends, of course, on radius. For instance, the escape velocity at the core radius of the same King model has been calculated to be 23 km s $^{-1}$. Since the rms velocities of the progenitors in the central parts of Sculptor are ~ 8.8 km s $^{-1}$, kick velocities of $\sqrt{23^2 - 8.8^2} \sim 21.5$ km s $^{-1}$ are enough for a LMXB formed at a core radius to be expelled. Consequently, if the centers of mass of all LMXBs have a recoil velocity of 21.5 km s $^{-1}$, a fraction of them are retained and the rest becomes unbound, depending on the location where the kick occurs. Since the fraction of mass within the core radius is 35%, a significant fraction ($\sim 65\%$) of the new formed LMXBs will escape for a kick velocity of 21.5 km s $^{-1}$ (a statistical approach to infer the mean kick velocity is given in Appendix D, reaching the same result).

The systems that survive as binaries and become LMXB progenitors attain a system velocity of 180 ± 80 km s $^{-1}$, if the distribution of angles between the kick velocity and the orbital plane of the presupernova binary is isotropic. If the range of kick directions is restricted to a cone along the spin axis with an opening of 20° , LMXBs are launched with kick velocities of order 20–100 km s $^{-1}$ (e.g., Podsiadlowski et al. 2005). In this case and if the distribution of kick velocities were drawn randomly in the range 20–100 km s $^{-1}$, less than 2 percent of the LMXBs would be retained in Sculptor. The recent analysis of the Galactic pulsar proper-motion data by Arzoumanian et al. (2002) found evidence for a bimodal distribution, with $\sim 40\%$ of the pulsars contained in a Maxwellian component with a dispersion of ~ 90 km s $^{-1}$, and the remaining neutron stars in a Maxwellian component with a dispersion of ~ 500 km s $^{-1}$. With this probability distribution, the retention fraction is slightly larger but still less than 2.8%.

The presence of a heavy binary companion at the time of the supernova explosion will make the retention more likely (e.g., Davies & Hansen 1998). Pfahl et al. (2002)

consider the inclusion of binaries and conclude that the retention fraction is probably not larger than several percent when they apply a single Maxwellian fast kick mode at 200 km s^{-1} and a central escape speed of 50 km s^{-1} . Scaling down their results, this implies that the retention fraction in Sculptor is likely not larger than a few percent even assuming that the velocity kick distribution is described by a slow Maxwellian mode at about 90 km s^{-1} . It is therefore puzzling to understand how Sculptor was able to hold on to most of its X-ray binaries in MOND theory.

One possibility is to invoke dark matter in MOND. Even if Sculptor obeys MOND, it can also contain a dark matter halo more extended than the optical galaxy such that the kinematics within the visible extent of Sculptor dwarf would not be greatly affected, but will be very effective at holding on to the LMXBs in the dSph potential. In this model, the MOND paradigm lowers the discrepancy between the binding mass and the baryonic mass but it still requires a total mass-to-light ratio $(M/L)_M \gtrsim 120$, where we have used Eq. (4) with $(M/L)_N \gtrsim 600$ (Dehnen & King 2006). Again, the inclusion of a dark halo in MOND weakens its appeal.

3.3. Compact early conditions

It is simple to see that if the stellar distribution was significantly more compact in the past than it is at present, the probability of old LMXBs to be bound to the potential increases. This is true for both Newtonian and MOND dynamics, but applies only if the compact dSph was subsequently heated to its current condition by a slow adiabatic process. A dSph galaxy could have been more massive in the past since mass-loss events can be caused by ram pressure stripping, supernovae explosions and tidal stripping. However, since these mechanisms are thought to be sudden and violent, it is very unlikely that they are able to produce the desired effect. While Read & Gilmore (2005) have simulated the dynamical effects of mass loss on the remaining stars and dark matter in the Newtonian case, it is illustrative to see that, in fact, the velocity dispersion of baryons is not altered enough to consider mass loss as a promising alternative possibility to explain the retention of observed LMXBs. In the recent simulations by Mayer et al. (2007), the formation of the darkest dSphs like Draco and Ursa Minor, is the result of the transformation from a gas-rich dwarf to a dSph by repeated tidal shocks at pericenters when the gas is readily removed by ram pressure stripping. Again, these impulsive shocks are not able to change the stellar properties in an adiabatic way. In this scenario, dSphs that fall into the Milky Way halo late, suffer little central stripping and may have periodic bursts of star formation because of funneling of this gas by a tidally-induced bar.

In the dark matter picture, there might exist another somewhat speculative way to produce dynamical heating of the stellar population. If the dark matter component is made up by massive black holes, gravitational encounters with stars will produce a transfer of energy between black holes and stars, in the attempt to reach equipartition. Jin, Ostriker & Wilkinson (2005) have demonstrated that the dynamical heating of an initially compact stellar distribution might produce a remnant distribution similar

to those in dSphs for black hole masses in excess of $10^5 M_\odot$. LMXBs formed at early stages ($\gtrsim 3 \text{ Gyr}$ ago) could become bound to the potential well of the dSph galaxy. However, this scenario is highly unlikely (Hernandez et al. 2004; Sánchez-Salcedo & Lora 2007).

3.4. Comparison with the escape velocities within the dark matter paradigm

For a central line-of-sight velocity dispersion of $6.2 \pm 1.1 \text{ km s}^{-1}$ as measured in Sculptor, the central mass-to-light ratio in the classical Newtonian view was estimated to be 6–13 (Queloz et al. 1995; Westfall et al. 2006). Given its large uncertainties, this range of values is consistent or marginally larger than the stellar mass-to-light ratio expected for an old stellar population (Queloz et al. 1995). Nevertheless, its kinematics could be also compatible with Sculptor being hosted by an extended subhalo. In fact, a mass estimator for dark matter halos via the escape-velocity argument was used by Dehnen & King (2006). They construct diagnostic dark halo models with cumulative mass profiles described by a simple analytic formula, designed to explore the generic parameters required for retaining LMXBs in Sculptor. These halos have different core radii, but all satisfying that the dark mass within the visible galaxy, with a radius of $\sim 1.85 \text{ kpc}$, be $5 \times 10^7 M_\odot$. They find that no reasonable dark matter halo in Sculptor can retain all LMXBs with ejection velocities in the range 20–100 km s^{-1} . To hold on to LMXBs with ejection velocities of up to 60 km s^{-1} , a dark matter halo having a total radius of upwards of 15 kpc is required. LMXBs with lower ejection speeds are more easily retained and require dark matter halos with more conservative parameters.

In order to make the comparison with MOND as fair as possible, we have explored the parameter space that ensures that LMXBs are retained in Sculptor but using full King models for the dark halo of Sculptor. Consistent with the findings of Dehnen & King (2006), we find that no realistic halo model is sufficient to retain LMXBs having large ejection velocities. Given that these ejection velocities are expected in the range of 20–100 km s^{-1} (e.g., Podsiadlowski et al. 2005), and that the velocity dispersion in Sculptor is of only around 9 km s^{-1} , this conclusion is not surprising. Actually, for the dark mass limits within the visible galaxy coming from dynamical studies, and imposing halo total radii smaller than 15 kpc , little room for varying the King halo parameters remains. For reasonable parameters of the dark halo, escape velocities are always of order 30–40 km s^{-1} . Figure D3 shows one such mass model for Sculptor, with the upper panel giving the cumulative mass profile for the stars (also taken as a King distribution with a stellar mass-to-light of 1.5 and a concentration of 0.63), and the total mass. The dominance of the dark matter halo is dramatic, especially at large radii, although not extraordinary in comparison to inferences of large galaxies. The bottom panel gives the escape speed as a function of radius together with the components due to the stars and dark matter. We see that even at the very center, the escape velocity is of only 40 km s^{-1} , and drops to 30 km s^{-1} at a distance of around 0.3 kpc . One should perhaps expect the progenitors of LMXBs to have been located within the central 0.165 kpc of Sculptor, which defines the core radius of the stellar

populations. This leads to the conclusion that standard dynamics and a reasonable dark matter halo proposal for Sculptor can explain the retention of LMXBs, only for those having started with a relatively low $\leq 40 \text{ km s}^{-1}$ initial kick. This is a more satisfactory situation than in the MOND case. In order to keep neutron stars with kick velocities $\gtrsim 50 \text{ km s}^{-1}$ bound, an extraordinarily extended and massive halo with a very large core radius should be invoked. Additionally, if a large fraction of neutron stars in dwarfs were formed in binary systems, the retention of LMXBs in Sculptor could be more plausible, but not trivial, certainly not for all initial velocities in the theoretical ejection range of velocities, at least not with the restriction that the total $M/L \lesssim 35$ within 1.85 kpc. Therefore, the problem of explaining the large retention of LMXBs is not exclusive of GCs (e.g., Pfahl et al. 2002).

4. CONCLUSIONS

We have pushed the measurements of tidal radii in Galactic GCs and dSph galaxies attempting to distinguish between dark matter and MOND. Except for Pal 14, the predicted tidal radii of GCs are systematically larger than the observed nominal values. However, this is not enough to rule out MOND because after including properly all the uncertainties, we find that they are consistent with the observed values at a 1σ level. The importance of the Galactic tide on the survival of dSph galaxies has been also investigated. Assuming mass-to-light ratios compatible with a naked stellar population, the present dSph galaxies preserve their integrity except perhaps Sextans, which might be undergoing tidal disruption. We suggest that deep observations of Sextans might provide a further test of MOND.

Based on the most recent data and with the updated values of a_0 and M_G , the dynamical mass-to-light ratios inferred under Newtonian and MOND gravities have been derived and compiled to see if new data can definitively tell us what the law of gravity at small galactic scales is (~ 300 pc). Since the dynamical mass in MOND should be dominated by stars, it is worrying that it requires mass-to-light ratios $\gtrsim 12$ for those dSph galaxies with radially extended data right to the optical edge (Ursa Minor and Draco). We warn that Willman 1, Coma Berenice, Ursa Major and Boötes may be also problematic for MOND. In particular, preliminary estimates for Willman 1, Coma Berenice and Ursa Major suggest $M/L \gtrsim 20$, at the 95% confidence level, even when possible outliers that inflate the inferred velocity dispersion, and hence the mass-to-light ratio, are omitted. That MOND requires a fraction of dark matter

in clusters of galaxies is a well-established issue. Taken at face value, our results indicate that MOND needs also a dark component in dSph galaxies with a mass fraction much beyond that required in galaxy clusters, weakening the appeal of the MOND paradigm, although this fact by itself does not rule out MOND as the gravity law at low accelerations.

An estimate of the mass of Sculptor has been given via the escape-velocity argument; LMXBs are ideal probes of the total mass as they should penetrate well outside the visible galaxy due to their high recoil velocities $\gtrsim 20 \text{ km s}^{-1}$. In the standard dark matter scenario, LMXBs with velocities $\gtrsim 40 \text{ km s}^{-1}$ are difficult to be retained for reasonable parameters of the dark halo. Hence, the well-known retention problem of LMXBs in GCs persists in dSphs. In the MONDian case, we have calculated that the mean square kick velocity of a presupernova binary to acquire the escape velocity is $\sim 24 \text{ km s}^{-1}$ in Sculptor. About 95% of the formed LMXBs would have escaped and been stripped from the Sculptor galaxy. In order for Sculptor to hold on to LMXBs with kick velocities of 50 km s^{-1} , a mass-to-light ratio $\gtrsim 120$ is required even under MOND hypothesis, making it structurally different. Therefore, either this is new evidence for the necessity of an extended dark halo in a galaxy in MOND, or the conventional thinking regarding neutron stars kicks must be modified. Measuring the radial velocities of the observed LMXBs would provide an obvious test of alternative gravities. High radial velocities $\gtrsim 30 \text{ km s}^{-1}$ may confirm the presence of a very massive dark matter halo much more extended than the stellar population.

Finally, one could argue that the large values of the M/L in MOND must be attributed to a problem with the velocity dispersion measurements and their estimated uncertainties. The required change in the velocity dispersions appears unlikely on purely statistical grounds and, in addition, they do not act in a systematic manner in Draco and Ursa Minor when compared to Sculptor.

In a MOND universe, data for several of these systems imply the presence of an extended dark matter halo. Although not a disproof of MOND, it does reduce the appeal of MOND significantly.

We would like to thank the anonymous referee for a careful reading of the manuscript and useful suggestions which improved the presentation of our final version. The authors acknowledge support from PAPIIT project IN-114107-3.

APPENDIX

MOND IN THE QUASI-NEWTONIAN LIMIT: VIRIAL THEOREM

For a satellite galaxy embedded in a constant external field g_{ext} , the gravitational field equation that governs the kinematics of the stellar component in the quasi-Newtonian limit is

$$\left(\nabla^2 + \frac{\partial^2}{\partial z^2}\right)\Phi = \frac{a_0}{g_{\text{ext}}}4\pi G\rho. \quad (\text{A1})$$

The solution of this modified Poisson equation for a distribution of mass $\rho(\vec{r})$ is given by

$$\Phi(\vec{r}) = -\left(\frac{Ga_0}{g_{\text{ext}}}\right)\int\frac{\rho(\vec{r}')}{\sqrt{2(x'-x)^2+2(y'-y)^2+(z'-z)^2}}d^3\vec{r}'. \quad (\text{A2})$$

As usual, the virial theorem for a stationary system can be derived after integration over an arbitrary volume \tilde{V} :

$$\int_{\tilde{V}} \rho v^2 d^3\vec{r} = \int_{\tilde{V}} \rho \vec{r} \cdot \vec{\nabla} \Phi d^3\vec{r}. \quad (\text{A3})$$

Substituting Eq. (A2) into Eq. (A3), one gets:

$$2K + W = 0, \quad (\text{A4})$$

where K is the total kinetic energy of the system and W is the system's total potential energy:

$$W \equiv \frac{1}{2} \int \rho(\vec{r}) \Phi(\vec{r}) d^3\vec{r}. \quad (\text{A5})$$

We have seen that the virial theorem has the same form than in the Newtonian case, with Φ as given by Eq. (A2).

POTENTIAL ENERGY OF A HOMOGENEOUS SPHERE IN THE QUASI-LINEAR LIMIT

We wish to calculate the potential energy, W , of a homogeneous sphere of constant density ρ and radius r_0 in the quasi-linear MONDian limit. According to Eq. (A5), we need Φ in order to evaluate W . The field equation (A1), can be transformed into the standard Poisson equation by making the substitution $z' = z/\sqrt{2}$:

$$\tilde{\nabla}^2 \Phi' = \frac{a_0}{g_{\text{ext}}} 4\pi G \rho(x, y, \sqrt{2}z'), \quad (\text{B1})$$

where $\Phi' = \Phi(x, y, z')$ and $\tilde{\nabla}^2 = \partial^2/\partial x^2 + \partial^2/\partial y^2 + \partial^2/\partial z'^2$. The relationship between the potentials is $\Phi(x, y, z) = \Phi'(x, y, z/\sqrt{2})$. For a sphere of constant density, Φ' satisfies:

$$\tilde{\nabla}^2 \Phi' = \frac{a_0}{g_{\text{ext}}} 4\pi G \rho', \quad (\text{B2})$$

where $\rho' = \rho$ within the ellipsoidal body bounded by the surface $r_0^2 = R^2 + 2z'^2$, which is an oblate ellipsoid with eccentricity $e = 0.71$. We are now in a position to calculate $W' = 1/2 \int \rho' \Phi' d^3\vec{r}'$ taking advantage of the theory of homoeoids (e.g., Roberts 1962; Binney & Tremaine 1987):

$$W' = -\frac{8}{15\sqrt{2}} \pi^2 \left(\frac{a_0}{g_{\text{ext}}} \right) G \rho^2 r_0^5 I(e), \quad (\text{B3})$$

with $I(e)$ an analytic function of the eccentricity as given in Table 2-2 of Binney & Tremaine (1987), being $I = 1.57$ for $e = 0.71$.

Finally, we can obtain W , $W = 1/2 \int \rho \Phi d^3\vec{r}$, in terms of W' by expressing W in terms of the new variable of integration $z \rightarrow z'$. This leads to $W = \sqrt{2}W'$. Substituting the value of W' from Eq. (B3) as a function of the total mass $M = 4\pi\rho r_0^3/3$, we find

$$W = -0.47 \left(\frac{a_0}{g_{\text{ext}}} \right) \frac{GM^2}{r_0}. \quad (\text{B4})$$

If the MOND dilation along the (x, y) -directions were ignored and the potential were assumed to be isotropic rather than anisotropic, the potential energy would be $-0.6(a_0/g_{\text{ext}})GM^2/r_0$. Hence, the error made using the isotropic approximation is 28%, for a homogeneous sphere.

DYNAMICAL MASS-TO-LIGHT RATIOS OF DSPHS

The closest and faintest dwarf in our sample is Willman 1 at a distance of 40 kpc and with a luminosity of $\sim 855 L_{\odot}$ (Martin et al. 2007). For the reported core radius of 16.6 pc, this galaxy may be treated as isolated for internal velocity dispersions $\gtrsim 2.7 \text{ km s}^{-1}$, corresponding to masses of $8.5 \times 10^4 M_{\odot}$. Therefore, for realistic mass-to-light ratios of a stellar population, Willman 1 is in the quasi-linear regime. The expected velocity dispersion is:

$$\sigma = 0.36 \sqrt{\frac{a_0}{g_{\text{ext}}}} \sqrt{\frac{GM}{r_{hp}}}, \quad (\text{C1})$$

where r_{hp} is the projected half-mass radius (e.g., Baumgardt et al. 2005). Suppose for a moment that the mass-to-light ratio is ~ 3 . Under this assumption, Eq. (C1) implies $\sigma = 0.53 \pm 0.1 \text{ km s}^{-1}$, where $r_{hb} \approx 21 \pm 7 \text{ pc}$ was used. By contrast, Martin et al. (2007) measure a radial velocity dispersion of $4.3 \pm_{1.3}^{2.3} \text{ km s}^{-1}$ and higher than 2.1 km s^{-1} at the 99% confidence limit. Therefore, if Willman 1 does not contain dark matter, it is already gravitationally unbound even under MOND, and will disperse in a few crossing-times, i.e. in a few $\sim 10^7 \text{ yr}$. This is at odds with the photometric data that do not show tidal tails or visible increase of the velocity dispersion with distance (Martin et al. 2007). Thus it would seem that Willman 1 needs a dark matter halo even in MOND.

In order for Willman 1 to be in virial equilibrium with a velocity dispersion of $\sim 4.3 \text{ km s}^{-1}$, we require a mass-to-light ratio between 370 and 550. This estimate was derived from the Newtonian values reported in Martin et al. (2007) but noting that since the system is not in deep MOND in this case (the internal accelerations are of the order of a_0), the MOND M/L value is only a factor of ~ 1.3 smaller than the Newtonian values (Milgrom 1994). Adopting the lower limit of 2.1 km s^{-1} at the 99% confidence level, Willman 1 lies in the quasi-linear deep-MOND regime and then $(M/L)_M > 30$.

For the new Galactic dSph candidate found in the constellation of Boötes, Martin et al. (2007) have derived a velocity dispersion $6.5 \pm_{1.3}^{2.1}$ km s⁻¹ from 24 members of the Boötes dwarf. For the adopted distance of 60 kpc, this galaxy has a core radius of ~ 225 pc and is well in the quasi-Newtonian regime. Adopting a total luminosity of $1.6 \times 10^4 L_\odot$ to $8.6 \times 10^4 L_\odot$, implies $(M/L)_{0,M} \sim 120$ to 23. Given the uncertainties in the velocity dispersion, $(M/L)_{0,M} \gtrsim 15$ at the 68% confidence. We must stress here that the magnitude and associated errors in the velocity dispersion and structural parameters of Boötes and Willman 1 are currently crude estimates.

For Ursa Minor, Wilkinson et al. (2004) derived a line-of-sight rms dispersion of 12 km s⁻¹, with $\sigma > 9.5$ km s⁻¹ at the 95% confidence level. A robust estimate of the total mass can be found from Eq. (3) provided that the velocity distribution is isotropic. For a value of $\sigma = 12$ km s⁻¹ we get $(M/L)_M = 60$ even taking the luminosity derived by Palma et al. (2003), while $(M/L)_M > 23$ at the 95% confidence level.

Based on the Newtonian value $(M/L)_N = 9$ and in the quasi-Newtonian limit (Eq. 4) with $g_{\text{ext}} = V^2/D$ and $V = 170$ km s⁻¹, the global $(M/L)_M$ in Sculptor is 1.0 ± 0.5 , for the observed central line-of-sight velocity dispersion 6.2 ± 1.1 km s⁻¹ (Queloz et al. 1995; Westfall et al. 2006). The real global M/L ratios are probably a factor $\times 2$ larger because the velocity dispersion shows a rise, leading to a mean velocity dispersion in the core of 8.8 ± 0.6 km s⁻¹ (Westfall et al. 2006). In any case, the mass-to-light ratios in MOND are perfectly consistent with an old stellar population. In a Newtonian dark matter view, a flat velocity-dispersion profile well beyond the several core radius, as occurs in Sculptor, is interpreted as the presence of a halo that begins to dominate dynamics increasingly outwards. However, in the MOND quasi-Newtonian limit, such a behavior for the velocity dispersion, even if the actual values of the stellar mass-to-light ratios remain within plausible ranges, would imply a radial change in the intrinsic properties of the stars, something hard to explain in such small systems, or that the dwarf galaxy is being heated by Galactic tides.

Draco and Fornax were studied by Lokas (2001, 2002). The $(M/L)_M$ values for isotropic models after updating by a_0 and the luminosities are 29 ± 9 and 2.2 ± 0.4 , respectively. The mass of Leo II and Leo I have been estimated with Eq. (3) using the mean velocity dispersion 6.6 ± 0.7 km s⁻¹ (Koch et al. 2007b) and 9.9 ± 1.5 km s⁻¹ (Koch et al. 2007a), respectively. For Carina, we estimate $(M/L)_M$ with Eq. (5) adopting the central value 6.97 ± 0.65 km s⁻¹ (Muñoz et al. 2006a).

For Sextans, the two-component models by Kleyna et al. (2004) suggest $(M/L)_N$ between 60–300 within 1 kpc, being the exact value sensitive to the form assumed for the outer fall-off in the velocity dispersion profile. Based on these Newtonian values, assuming that the external field is dominant in Sextans, a $(M/L)_M$ of ~ 7.5 –36 was found when adopting a distance of 86 kpc. Although M/L of GCs have a 3σ range of 1–4.3 (Feltzing et al. 1999; Parmentier & Gilmore 2001), values as high as 7–8 cannot be ruled out for a stellar old population (Queloz et al. 1995; Romanowsky et al. 2003). Hence, a mass-to-light ratio of ~ 8 seems to be compatible with its kinematics and might be associated to a naked stellar old component.

In the case of the recently discovered Ursa Major dSph, for a central velocity dispersion of 7.6 km s⁻¹ and a core radius $r_c \sim 200$ pc (Simon & Geha 2007), we obtain a central mass-to-light ratio of 135 in the isolated limit. For the value reported by Martin et al. (2007), $\sigma = 11.9 \pm_{2.3}^{3.5}$ km s⁻¹, the mass-to-light ratio is even larger. The velocity dispersion is in fact greater than 6.0 km s⁻¹ at a 95% confidence level. Adopting this lower value, Ursa Major lies in the quasi-Newtonian regime and, then, $(M/L)_{0,M} > 52$ with 95% confidence. The magnitude of Ursa Major is currently a crude estimate. Improving the data on this galaxy is key to exploring how MOND behaves at the smallest galactic scales (~ 300 pc).

Measurements of the velocity dispersions for Coma Berenices, Hercules and Canes Venatici II were reported in Simon & Geha (2007). They measure the velocities of 59 stars in Coma Berenice, obtaining a velocity dispersion 4.6 ± 0.8 km s⁻¹. Equation (5) with $r_c = 41$ pc and $(M/L)_N = 448$ implies a MOND mass-to-light ratio of 105. Hercules is likely dominated by the external acceleration because $\eta \simeq 0.91$ for $r_c = 205$ pc and assuming a distance of 140 kpc. For a velocity dispersion 5.1 ± 0.9 km s⁻¹ and $(M/L)_N = 332$, we obtain $(M/L)_{0,M} = 26 \pm_9^{11}$. Finally, the ultra-faint Canes Venatici II is located at 150 kpc. We have used $r_c = 84$ pc and $\sigma = 4.6 \pm 1$ km s⁻¹ to infer $(M/L)_{0,M} = 38.5 \pm_{24}^{46}$.

Since the global luminosity is less certain than the central luminosity, we can use the central mass-to-light estimators $(M/L)_{0,M}$ as a check of the robustness of the estimates, for Draco and Ursa Minor. Assuming that mass follows light, Odenkirchen et al. (2001) obtain $(M/L)_N = 146$ for Draco. If we take this value as representative of the Newtonian value within the optical radius of Draco, and for a central velocity dispersion $\sigma_0 = 8$ km s⁻¹ (Lokas et al. 2006) and core radius of 180 pc, Eq. (5) gives $(M/L)_{0,M} = 24^2$. In the case of Ursa Minor, the central Newtonian value is 100 after updating the quoted value of Mateo (1998) with the latest determination of $\sigma_0 = 12$ km s⁻¹ (Wilkinson et al. 2004), instead of 9.3 km s⁻¹ adopted in Mateo (1998). From Eq. (5) with $r_c = 200$ pc, we get $(M/L)_{0,M} = 33$. These central values of $(M/L)_{0,M}$ are therefore in agreement with the global estimates.

MEAN SQUARE KICK VELOCITY TO ESCAPE

Consider a progenitor system of a LMXB, which is embedded in a galaxy that lies in the quasi-Newtonian regime in MOND. If the progenitor system is moving at velocity \vec{v} and the supernova explosion occurs at \vec{r} , then the minimum kick velocity for the new formed LMXB to become gravitationally unbound, \vec{v}_k , satisfies:

$$\frac{1}{2} (\vec{v} + \vec{v}_k)^2 + \Phi(\vec{r}) - \frac{1}{2} |\vec{\Omega} \times \vec{r}|^2 = \Phi(\vec{r}_t) - \frac{1}{2} |\vec{\Omega} \times \vec{r}_t|^2, \quad (\text{D1})$$

² Milgrom (1995) obtained a central $M/L = 4$, using $\sigma_0 = 9.2$ km s⁻¹ and $a_0 = 2 \times 10^{-8}$ cm s⁻².

where $\vec{\Omega}$ is the angular velocity of the dwarf satellite around its parent galaxy, $\vec{r}_t = (0, 0, r_t)$ and r_t the tidal radius along the line pointing the centers of the galaxies. The mean square kick velocity for stars to escape is:

$$\langle v_k^2 \rangle = -\langle v^2 \rangle - 2(\langle \Phi(\vec{r}) \rangle - \Phi(\vec{r}_t)) + \langle |\vec{\Omega} \times \vec{r}|^2 \rangle - |\vec{\Omega} \times \vec{r}_t|^2, \quad (\text{D2})$$

where the brackets represent the mass average:

$$\langle a \rangle \equiv \frac{\int \rho(\vec{r}) a d^3 \vec{r}}{\int \rho(\vec{r}) d^3 \vec{r}} = \frac{1}{M_{dw}} \int \rho(\vec{r}) a d^3 \vec{r}. \quad (\text{D3})$$

In Eq. (D2) we used $\langle \vec{v} \cdot \vec{v}_k \rangle = 0$ for an isotropic distribution of kick directions.

In the quasi-Newtonian MOND regime, Equation (D2) can be expressed in terms of observable quantities as follows. First, the quantity $\langle |\vec{\Omega} \times \vec{r}|^2 \rangle$ is exactly $2\Omega^2 \langle r^2 \rangle / 3$ for a spherical distribution of matter. Corrections for non-sphericity of the distribution in the central parts of the dwarf satellite were found to be unimportant as far as $\langle v_k^2 \rangle$ concerns. Ignoring the variation of the external gravitational field in the vicinity of the satellite, $\langle v_k^2 \rangle$ can be written:

$$\langle v_k^2 \rangle = -\frac{2K}{M_{dw}} - \frac{4W}{M_{dw}} + 2\Phi(\vec{r}_t) + \Omega^2 \left(\frac{2}{3} \langle r^2 \rangle - r_t^2 \right), \quad (\text{D4})$$

where K is the total kinetic energy of the stellar system and W the total potential energy³ (Appendix A). It is easy to show that, independently of the concentration, $\langle r^2 \rangle < r_t^2 / 5$ in any King model. Using the virial theorem in the quasi-linear regime (see Eq. A4), with $K = 3M_{dw}\sigma^2/2$, σ the global one-dimensional velocity dispersion, $\Omega = V/D$ and approximating $\Phi(\vec{r}_t) \approx -G(a_0/g_{\text{ext}})M_{dw}/r_t$, it holds that:

$$\langle v_k^2 \rangle \leq 9\sigma^2 - 2\frac{a_0}{g_{\text{ext}}} \frac{GM_{dw}}{r_t} - \frac{13}{15} \left(\frac{r_t}{D} \right)^2 V^2. \quad (\text{D5})$$

The second term of the RHS can be expressed in terms of σ exploiting again the virial theorem and noting that the potential energy in a King model with $W_0 = 4$ is $|W| = (9/5)GM_{dw}^2/r_t$ in Newtonian dynamics (King 1966), which translates into an upper limit in MOND due to the dilation factor (Eq. A2), i.e. $|W| < (9/5)G(a_0/g_{\text{ext}})M_{dw}^2/r_t$. Consequently,

$$\langle v_k^2 \rangle \leq 8\sigma^2 - \frac{13}{15} \left(\frac{r_t}{D} \right)^2 V^2. \quad (\text{D6})$$

For the parameters of Sculptor: $\sigma \simeq 0.95\sigma_c = 8.4 \text{ km s}^{-1}$, $r_t = 1.8 \text{ kpc}$, $V = 170\text{--}185 \text{ km s}^{-1}$, $D \simeq 79 \text{ kpc}$, we obtain $\langle v_k^2 \rangle^{1/2} \lesssim 23.5 \text{ km s}^{-1}$.

REFERENCES

- Allen, C., Moreno, E., & Pichardo, B. 2006, *ApJ*, 652, 1150
 Armandroff, T. E., Olszewski, E. W., & Pryor, C. 1995, *AJ*, 110, 2131
 Arzoumanian, Z., Chernoff, D. F., & Cordes, J. M. 2002, *ApJ*, 568, 289
 Baumgardt, H., Grebel, E. K., & Kroupa, P. 2005, *MNRAS*, 359, L1
 Begeman, K. G., Broeils, A. H., & Sanders, R. H. 1991, *MNRAS*, 249, 523
 Bekenstein, J., & Milgrom, M. 1984, *ApJ*, 286, 7
 Bellazzini, M. 2004, *MNRAS*, 347, 119
 Bellazzini, M., Gennari, N., & Ferraro, F. R. 2005, *MNRAS*, 360, 185
 Belokurov, V. et al. 2006, *ApJ*, 647, L111
 Belokurov, V. et al. 2007, *ApJ*, 654, 897
 Binney, J., & Tremaine, S. 1987, *Galactic Dynamics* (Princeton: Princeton Univ. Press)
 Bottema, R., Pestaña, J. L. G., Rothberg, B., & Sanders, R. H. 2002, *A&A*, 393, 453
 Burkert, A. 1997, *ApJ*, 474, L99
 Cacciari, C. 1999, in *Harmonizing Cosmic Distance Scales in a Post-Hipparcos Era*, ASP Conf. Ser. Vol. 167, eds. D. Egret & A. Heck, (San Francisco: ASP), p. 140
 Clementini, G., Ripepi, V., Bragaglia, A., Fiorenzano, A. F. M., Held, E. V., & Gratton, R. G. 2005, *MNRAS*, 363, 734
 Ciotti, L., & Binney, J. 2004, *MNRAS*, 351, 285
 Davies, M. B., & Hansen, B. M. S. 1998, *MNRAS*, 301, 15
 Dehnen, W., & Binney, J. 1998, *MNRAS*, 294, 429
 Dehnen, W., & King, A. 2006, *MNRAS*, 367, L29
 Faber, S. M., & Lin, D. N. C. 1983, *ApJ*, 266, L17
 Famaey, B., & Binney, J. 2005, *MNRAS*, 363, 603
 Famaey, B., Bruneton, J.-P., & Zhao H. 2007, *MNRAS*, 377, L79
 Feltzing, S., Gilmore, G., & Wyse, R. F. G. 1999, *ApJ*, 516, L17
 Gerhard, O. E. 1994, in *Proc. of ESO/OHP Workshop of Dwarf Galaxies*, ed. G. Meylan & P. Prugniel (Garching: ESO), 335
 Gerhard, O. E., & Spiegel, D. N. 1992, *ApJ*, 397, 38
 Gnedin, O. Y., Lee, H. M., & Ostriker, J. P. 1999, *ApJ*, 522, 935
 Harris, W. E. 1996, *AJ*, 112, 1487
 Heggie, D. C., & Ramamani, N. 1995, *MNRAS*, 272, 317
 Hernandez, X., Gilmore, G., & Valls-Gabaud, D. 2000, *MNRAS*, 317, 831
 Hernandez, X., Matos, T., Sussman, R. A., & Verbin, Y. 2004, *Phys. Rev. D*, 70, 043537
 Hilker, M. 2006, *A&A*, 448, 171
 Ibata, R., Chapman, S., Irwin, M., Lewis, G., & Martin, N. 2006, *MNRAS*, 373, L70
 Illingworth, G. 1976, *ApJ*, 204, 73
 Innanen, K. A., Harris, W. E., Webbink, R. F. 1983, *AJ*, 88, 338
 Irwin, M., & Hatzidimitriou, D. 1995, *MNRAS*, 277, 1354
 Jin, S., Ostriker, J. P., & Wilkinson, M. I. 2005, *MNRAS*, 359, 104
 Keenan, D. W. 1981a, *A&A*, 95, 334
 Keenan, D. W. 1981b, *A&A*, 95, 340
 King, I. 1962, *AJ*, 67, 471
 King, I. 1966, *AJ*, 71, 64
 Kleyna, J. T., Wilkinson, M. I., Evans, N. W., & Gilmore, G. 2001, *ApJ*, 563, L115
 Kleyna, J. T., Wilkinson, M. I., Evans, N. W., Gilmore, G. 2004, *MNRAS*, 354, L66
 Kleyna, J. T., Wilkinson, M. I., Evans, N. W., & Gilmore, G. 2005, *ApJ*, 630, L141
 Koch, A., et al. 2007a, *ApJ*, 657, 241
 Koch, A., et al. 2007b, *ApJ*, in press (arXiv:0704.3437)
 Koposov, S. et al. 2007, submitted to *ApJ*(arXiv:0706.0019)
 Kroupa, P. 1997, *New Astron.*, 2, 139
 Kuhn, J. R., & Miller, R. H. 1989, *ApJ*, 341, L41
 Lokas, E. L. 2001, *MNRAS*, 327, L21
 Lokas, E. L. 2002, *MNRAS*, 333, 697

³ Note that the concept of total potential energy is not well-defined in an isolated system but it is meaningful in the quasi-Newtonian field limit.

- Lokas, E. L., Mamon, G. A., Prada, F., 2006, in *Mass Profiles and Shapes of Cosmological Structures*, eds. G. Mamon, F. Combes, C. Deffayet, B. Fort, (EAS Publ. Ser., Paris), Vol. 20, p. 113
- Maccarone, T. J., Kundu, A., Zepf, S. E., Piro, A. L., & Bildsten, L. 2005, *MNRAS*, 364, L61
- Martin, N. F., Ibata, R. A., Chapman, S. C., Irwin, M., & Lewis, G. F. 2007, *MNRAS*, in press (arXiv:0705.4622)
- Mateo, M. 1998, *ARA&A*, 36, 435
- Mateo, M., Olszewski, E. W., Vogt, S. S., & Keane, M. J. 1998, *AJ*, 116, 2315
- Mayer, L., Kazantzidis, S., Mastrogiuseppe, C., & Wadsley, J. 2007, *Nature*, 445, 738
- McLaughlin, D. E., & Meylan, G. 2003, in *New Horizons in Globular Cluster Astronomy* eds. G. Piotto, G. Meylan, G. Djorgovski, M. Riello, *ASP Conf. Ser. Vol. 296*, (Astron. Soc. Pac., San Francisco), p. 153
- Milgrom, M. 1983, *ApJ*, 270, 365
- Milgrom, M. 1994, *ApJ*, 429, 540
- Milgrom, M. 1995, *ApJ*, 455, 439
- Muñoz, R. R., et al. 2006a, *ApJ*, 649, 201
- Muñoz, R. R., et al. 2006b, *ApJ*, 650, L51
- Odenkirchen, M., et al. 2001, *AJ*, 122, 2538
- Oh, K. S., & Lin, D. N. C. 1992, *ApJ*, 386, 519
- Oh, K. S., Lin, D. N. C., & Aarseth, S. J. 1992, *ApJ*, 386, 506
- Oh, K. S., Lin, D. N. C., & Aarseth, S. J. 1995, *ApJ*, 442, 142
- Olszewski, E. W., Pryor, C., & Shommer, R. B. 1993, in *The globular clusters-galaxy connection*, eds. G. H. Smith, J. P. Brodie, *Astronomical Society of the Pacific Conference Series*, Vol. 48, p. 99
- Palma, C., Majewski, S. R., Siegel, M. H., Patterson, R. J., Ostheimer, J. C., & Link, R. 2003, *AJ*, 125, 1352
- Parmentier, G., & Gilmore, G. 2001, *A&A*, 378, 97
- Pfahl, E., Rappaport, S., & Podsiadlowski, P. 2002, *ApJ*, 573, 283
- Piatek, S., & Pryor, C. 1995, *AJ*, 109, 1071
- Piatek, S., et al. 2006, *AJ*, 131, 1445
- Podsiadlowski, P., Pfahl, E., & Rappaport, S. 2005, in *Binary Radio Pulsars*, eds. F. A. Rasio, I. H. Stairs, *ASP Conf. Ser. 328*, p. 327
- Pryor, C. 1996, in *The Formation of the Halo - Inside and Out*, eds. H. Morrison, A. Sarajedini, *ASP Conf. Proc. 92*, (San Francisco: ASP), p. 424
- Pryor, C., & Meylan, G. 1993, in *Structure and Dynamics of Globular Clusters*, eds. S. G. Djorgovski, G. Meylan G., *Astronomical Society of the Pacific*, Vol. 50, (San Francisco, California), p. 357
- Queloz, D., Dubath, P., & Pasquini, L. 1995, *A&A*, 300, 31
- Read, J. I., & Gilmore, G. 2005, *MNRAS*, 356, 107
- Read, J. I., Wilkinson, M. I., Evans, N. W., Gilmore, G., & Kleyna, J. T. 2006, *MNRAS*, 367, 387
- Richstone, D. O., & Tremaine, S. 1986, *AJ*, 92, 72
- Roberts, P. H. 1962, *ApJ*, 136, 1108
- Romanowsky, A. J., Douglas, N. G., Arnaboldi, M., Kuijken, K., Merrifield, M. R., Napolitano, N. R., Capaccioli, M., & Freeman, K. C. 2003, *Science*, 301, 1696
- Sánchez-Salcedo, F. J., & Hidalgo-Gómez, A. M. 1999, *A&A*, 345, 36
- Sánchez-Salcedo, F. J., & Lora, V. 2007, *ApJ*, 658, L83
- Sánchez-Salcedo, F. J., Reyes-Iturbide, J., & Hernandez, X. 2006, *MNRAS*, 370, 1829
- Sanders, R. H., & McGaugh, S. S. 2002, *ARA&A*, 40, 263
- Simon, J. D., & Geha, M. 2007, submitted to *ApJ*(arXiv:0706.0516)
- Sohn, S. T., et al. 2006, *ApJ*, in press (arXiv:astro-ph/0608151v2)
- Spitzer, L. 1987, *Dynamical Evolution of Globular Clusters* (Princeton Series in Astrophysics: Princeton University Press)
- Tolstoy, E., et al. 2004, *ApJ*, 617, L119
- Trager, S. C., King, I. R., & Djorgovski, S. 1995, *AJ*, 109, 218
- Vogt, S. S., Mateo, M., Olszewski, E. W., & Keane, M. J. 1995, *AJ*, 109, 151
- Wakamatsu, K.-I. 1981, *PASP*, 93, 707
- Walcher, C. J., Fried, J. W., Burkert, A., & Klessen, R. S. 2003, *A&A*, 406, 847
- Walker, M. G., Mateo, M., Olszewski, E. W., Bernstein, R., Wang, X., & Woodroffe, M. 2006, *AJ*, 131, 2114
- Westfall, K. B., Majewski, S. R., Ostheimer, J. C., Frinchaboy, P. M., Kunkel, W. E., Patterson, R. J., & Link, R. 2006, *AJ*, 131, 375
- Wilkinson, M. I., Kleyna, J. T., Evans, N. W., Gilmore, G. F., Irwin, M. J., & Grebel, E. K. 2004, *ApJ*, 611, L21
- Zhao, H. 2005, *A&A*, 444, L25
- Zhao, H., & Tian, L. 2006, *A&A*, 450, 1005

TABLE D1

A SUMMARY OF RELEVANT PARAMETERS FOR THE CLOSEST dSPH GALAXIES. THE SECOND (AND THIRD) ROW FOR SOME OF THE OBJECTS GIVES THE VALUES REPORTED BY OTHER AUTHORS.

Galaxy	L $10^5 L_\odot$	r_t arcmin	$(M/L)_N^a$	Comp. ^b	F_N	$(M/L)_M^c$	F_M	References for $(L, r_t, (M/L)_N)$
Willman 1	0.0085	~ 7.4	500	1	0.25	$\gtrsim 30(95\%)$	0.36	M07, M07, M07
Coma Ber.	0.027	—	$448 \pm_{142}^{169}$	1	—	$\gtrsim 46(95\%)$	—	B06, —, S07
Boötes	0.86	—	130	1	—	$23 \pm_8^{17}$	—	M06b, —, M07
Ursa Minor	2.9	50.6 ± 3.6	79 ± 39	1	0.55	12 ± 6	0.51	M98, IH95, M98
	5.8	77.9 ± 8.9	40 ± 20	1	0.85	6 ± 3	0.77	P03, P03, P03
	5.8	~ 34	340 ± 240	2	0.19	$\gtrsim 23(95\%)$	0.16	P03, W04, W04
Sculptor	14	79.6 ± 3.3	9 ± 6	1	1.13	1.0 ± 0.5	1.10	IH95, We06, Q95
	14	~ 60	9 ± 6	1	0.86	1.0 ± 0.5	0.83	IH95, We06, Q95
Draco	2.6	28.3 ± 2.4	$\gtrsim 240$	2	0.24	$\gtrsim 13(95\%)$	0.28	M98, IH95, K01
	2.4	$\gtrsim 40.1$	140 ± 40	1	0.42	$\gtrsim 12(95\%)$	0.40	O01, O01, O01
Sextans	5.0	160 ± 50	107 ± 72	1	1.40	22 ± 15	1.05	M98, IH95, IH95
Carina	4.3	28.8 ± 3.6	$43 \pm_{19}^{53}$	1	0.42	4.5 ± 0.9	0.35	M98, IH95, M06a
Ursa Major	0.15	—	1024 ± 636	1	—	$\gtrsim 52(95\%)$	—	B06, —, S07
Fornax	155	71.1 ± 4.0	15 ± 10	2	0.46	2.2 ± 0.4	0.33	M98, IH95, Wa06
	155	90	15 ± 10	2	0.58	2.2 ± 0.4	0.42	M98, W03, Wa06
Hercules	0.21	—	$332 \pm_{106}^{127}$	1	—	$26 \pm_9^{11}$	—	B07, —, S07
Canes Vn II	0.071	—	$336 \pm_{130}^{162}$	1	—	$38.5 \pm_{24}^{46}$	—	B07, —, S07
Leo II	7.5	8.7 ± 0.9	$35.6 \pm_{7.7}^{8.8}$	1	0.19	4.3 ± 2.1	0.09	M98*, IH95, K07b
Leo I	47.9	12.6 ± 1.5	17 ± 4	1	0.12	$3.4 \pm_{1.5}^{2.5}$	0.07	M98, IH95, K07a
	76	13.4 ± 0.7	5.3 ± 2.6	1	0.13	$2.1 \pm_{1.0}^{1.5}$	0.07	S06, S06, S06

^aMass-to-light ratios for the Galactic dSphs with determinations of their internal kinematics. The quoted 1σ error bars do not include the associated uncertainties in luminosity or distance. In galaxies in which the reported value of the luminosity varies significantly between different authors, we have added a second row. Obviously, in order to have low values of the M/L 's, the larger values of the luminosity should be taken.

^bWe indicate the mass model used. “1” indicates one-single King component models –with or without dark matter. If the velocity dispersion profile is available, the assumption that mass-follows-light can be relaxed and more reliable models can be obtained. “2” refers to models in which dark matter and stars follow different profiles (2-component models).

^cConfidence levels are given in parenthesis.

*Updated values using $D = 233$ kpc (Bellazzini et al. 2005).

Note. — agenda of the acronyms: B06: Belokurov et al. 2006; B07: Belokurov et al. 2007; IH95: Irwin & Hatzidimitriou 1995; K01: Kleyna et al. 2001; K05: Kleyna et al. 2005; K07a: Koch et al. 2007a; K07b: Koch et al. 2007b; M98: Mateo 1998; M06a: Muñoz et al. 2006a; M06b: Muñoz et al. 2006b; M07: Martin et al. 2007; O01: Odenkirchen et al. 2001; P03: Palma et al. 2003; Q95: Queloz et al. 1995; S06: Sohn et al. 2006; S07: Simon & Geha 2007; W03: Walcher et al. 2003; W04: Wilkinson et al. 2004; Wa06: Walker et al. 2006; We06: Westfall et al. 2006.

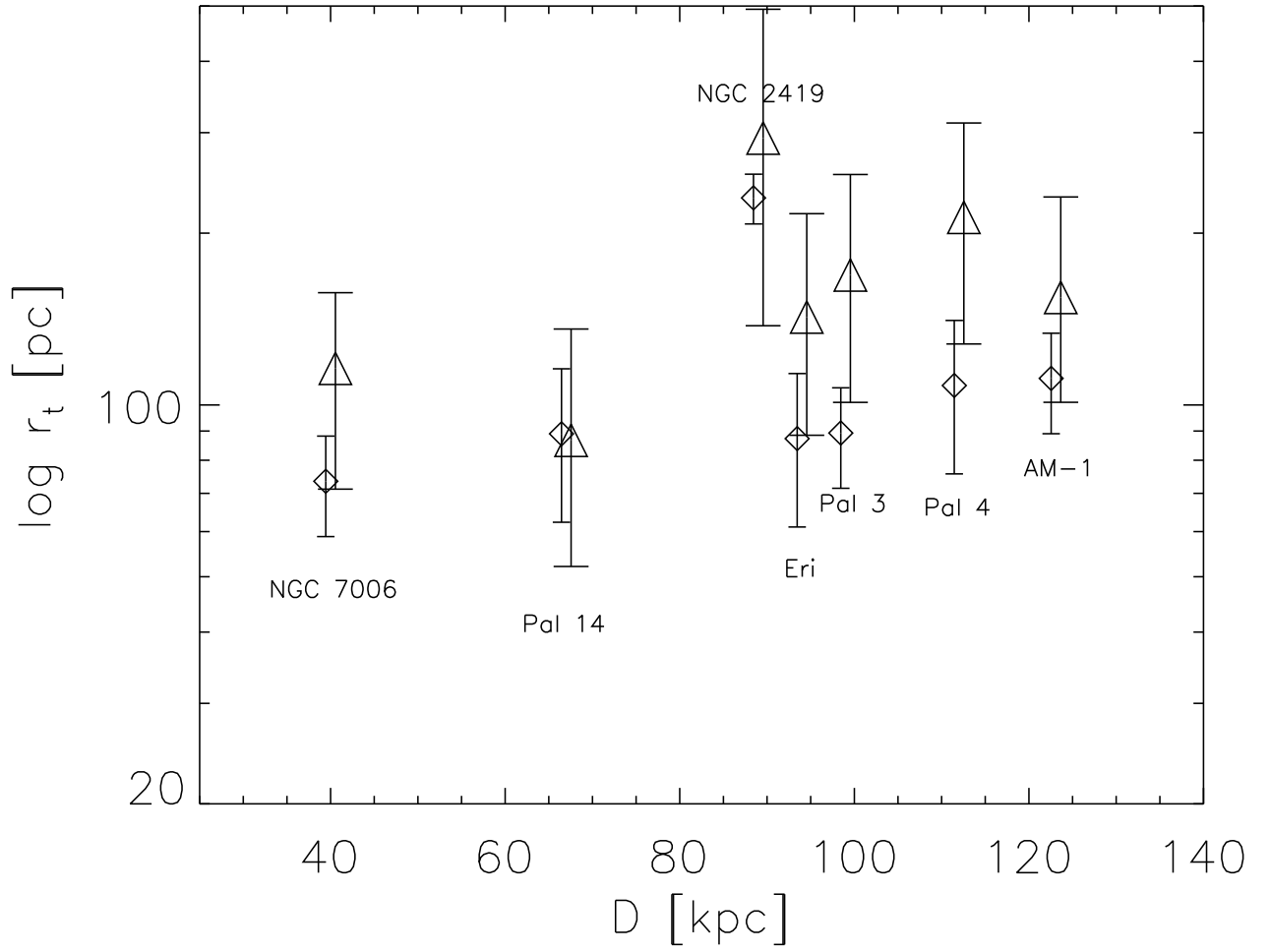


FIG. D1.— Comparison of tidal radii in MOND with $M_G = 0.7 \times 10^{11} M_\odot$ for remote GCs. The error bars enclose 1σ confidence limit range. The predicted tidal radii (triangles) are compared with the observed tidal radii (diamonds). The symbols have been shifted horizontally to make the plot readable. The observed limiting radii were taken from Harris & van den Bergh (1984) for Pal 14; Harris (1996) for NGC 7006, NGC 2419, Eri, and Pal 4; from Hilker (2006) for Pal 3 and AM-1.

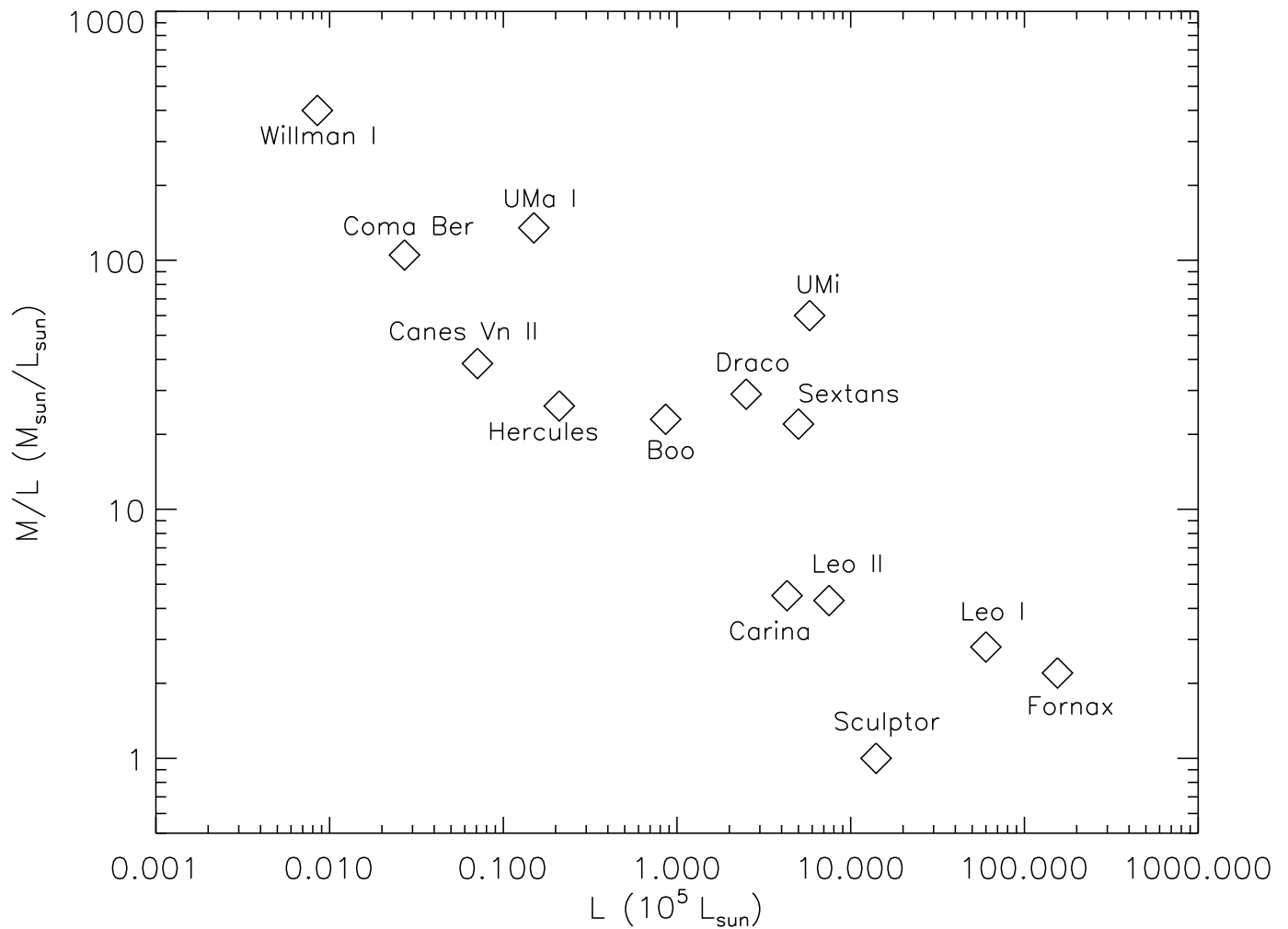


FIG. D2.— Inferred MONDian mass-to-light ratios versus luminosity for the known Galactic dSph galaxies at $40 < D < 260$ kpc and with velocity dispersion estimates (see text).

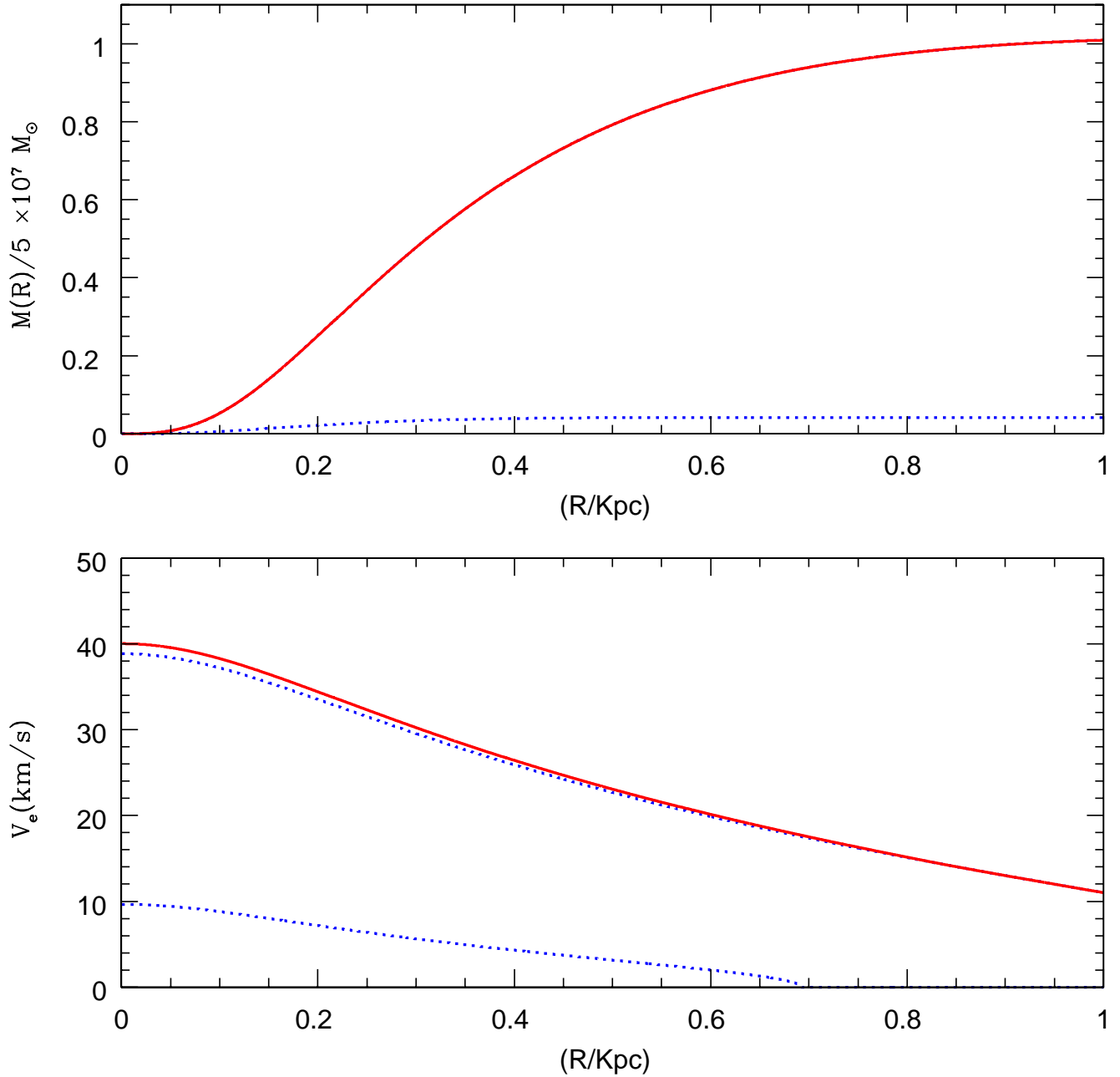


FIG. D3.— The upper panel shows a mass model for Sculptor constrained to agree with observed total stellar content and scale length (dotted curve), and a dark matter mass within 1.85 kpc of $5 \times 10^7 M_{\odot}$, compatible with the stellar velocity dispersion within this region. The core radius of the dark halo is ~ 0.3 kpc. The lower panel gives the contributions to the escape velocity at different radii, from stars (lower dotted curve), dark halo (upper dotted curve), and total (solid curve). The dynamics is entirely dominated by the dark matter halo, which can only retain LMXBs having a low initial kick.